



Tropical cyclone rainfall in the Mekong River Basin for 1983–2016

Aifang Chen^a, Chang-Hoi Ho^b, Deliang Chen^{a,c,*}, Cesar Azorin-Molina^{a,d}

^a Regional Climate Group, Department of Earth Sciences, University of Gothenburg, Gothenburg 40530, Sweden

^b School of Earth and Environmental Sciences, Seoul National University, Seoul 151-742, South Korea

^c CAS Center for Excellence in Tibetan Plateau Earth Sciences, Chinese Academy of Sciences, Beijing 100101, China

^d Centro de Investigaciones sobre Desertificación, Consejo Superior de Investigaciones Científicas (CIDE-CSIC), Montcada, Valencia, Spain



ARTICLE INFO

Keywords:

Tropical cyclones
Occurrence
Rainfall
Mekong River Basin

ABSTRACT

As home to about 70 million people, the Mekong River Basin (MRB), located in Mainland Southeast Asia, is often influenced by tropical cyclones (TCs) landfalling. The TCs not only cause flood and storm hazards, but also play important roles in providing freshwater resource and welcomed sediment transports. Our study focuses on the climatology of TCs and associated rainfall (TCR) in the MRB for 1983–2016. Results show that: (i) the mean landfall occurrence of TCs is 6.2 yr^{-1} , leading to 36.7 mm yr^{-1} of annual mean TCR (2.5% of the annual total precipitation), which mainly occur in monsoon-TC season (i.e., June–November); (ii) TCs highly concentrate on the lower eastern MRB, generating the largest TCR contribution of 12.4% to the annual total precipitation; (iii) the annual mean contribution of TCs induced extreme precipitation - R20mm and R50mm (days of heavy precipitation rate $\geq 20 \text{ mm day}^{-1}$ and $\geq 50 \text{ mm day}^{-1}$, respectively) - to that from annual total precipitation is large in the lower eastern MRB; (iv) over 60% of the basin area is influenced by TCR on average; and (v) a significant weakening trend of the TC frequency has been observed. The present findings lay a foundation for further in-depth research of the potential influence of the dynamic TCs and the associated rainfall in the MRB.

1. Introduction

As one of the most devastating natural hazards to the society, tropical cyclones (hereafter TCs) associated with flood, storm surge, and heavy rainfall often result in loss of human lives, health problems, and economic losses (Rappaport, 2000, 2014; Lin et al., 2015; Martin, 2015; Zhang et al., 2017). Assessed by the World Meteorological Organization (WMO), about 76% of the live losses caused by meteorological and hydrological hazards occurred in Asian region (e.g., India, Indochina, China, Japan, and Korea) in 1970–2012 were linked to TCs and intense low pressure systems (WMO, 2014; MRC, 2015). There are many well-known severe TCs in Asian countries, e.g., Fred (1994) in China, Rusa (2002) in South Korea, Pabuk (2007) in Vietnam, Nargis (2008) in Myanmar, and Haiyan (2013) in Philippines. Besides these harmful effects, TCs have positive hydro-climatic influences on the ecosystem and society (e.g., providing freshwater resource for agriculture), especially when the TCs associated rainfall (hereafter TCR) and wind ease heatwave and drought conditions in a warm summer (Dare et al., 2012; Khouakhi et al., 2017; Zhou and Matyas, 2017).

Located in Mainland Southeast Asia, the Mekong River is listed as the 10th longest river in the world, and the Mekong River Basin (hereafter MRB) supports for 70 million people from China, Myanmar,

Lao PDR, Thailand, Cambodia, and Vietnam (Fig. 1a) (MRC, 2010). Over 80% of the people live close to the river; the lower basin is also one of the world largest inland fishery (Ziv et al., 2012). Indeed, there is an increasing vulnerability of riparian countries to flood, which tends to cause fatalities and property damage, especially for those who live on the margins of economic development (MRC, 2015).

The complex climate in the MRB is of high spatiotemporal variability, shifting from temperate monsoon to tropical monsoon from the upper basin to lower basin. It is characterized by distinct monsoon (June–October) and non-monsoon (November–following May) seasons (MRC, 2010). TCs mainly influence the basin during the monsoon season, and it can partly cause the second peak of seasonal streamflow in September–November (Nguyen, 2008; Takahashi and Yasunari, 2008; MRC, 2010; Räsänen and Kumm, 2013). The incursion of TCs into the MRB is a major factor in the development of regional flood events (MRC, 2015; Chhin et al., 2016). Besides the abovementioned potential influence of TCs, they also play vital roles in mobilizing sediment of the Mekong River (Darby et al., 2013, 2016), where the river delta is facing serious land subsidence ($\sim 1.6 \text{ cm yr}^{-1}$) and sea level rise (Erban et al., 2014).

Previous studies have focused on TCs and TCR over the past decades across the Indochina Peninsula (Takahashi and Yasunari, 2008; Chhin

* Corresponding author at: Regional Climate Group, Department of Earth Sciences, University of Gothenburg, Box 460, 40530 Gothenburg, Sweden.
E-mail address: deliang@gvc.gu.se (D. Chen).

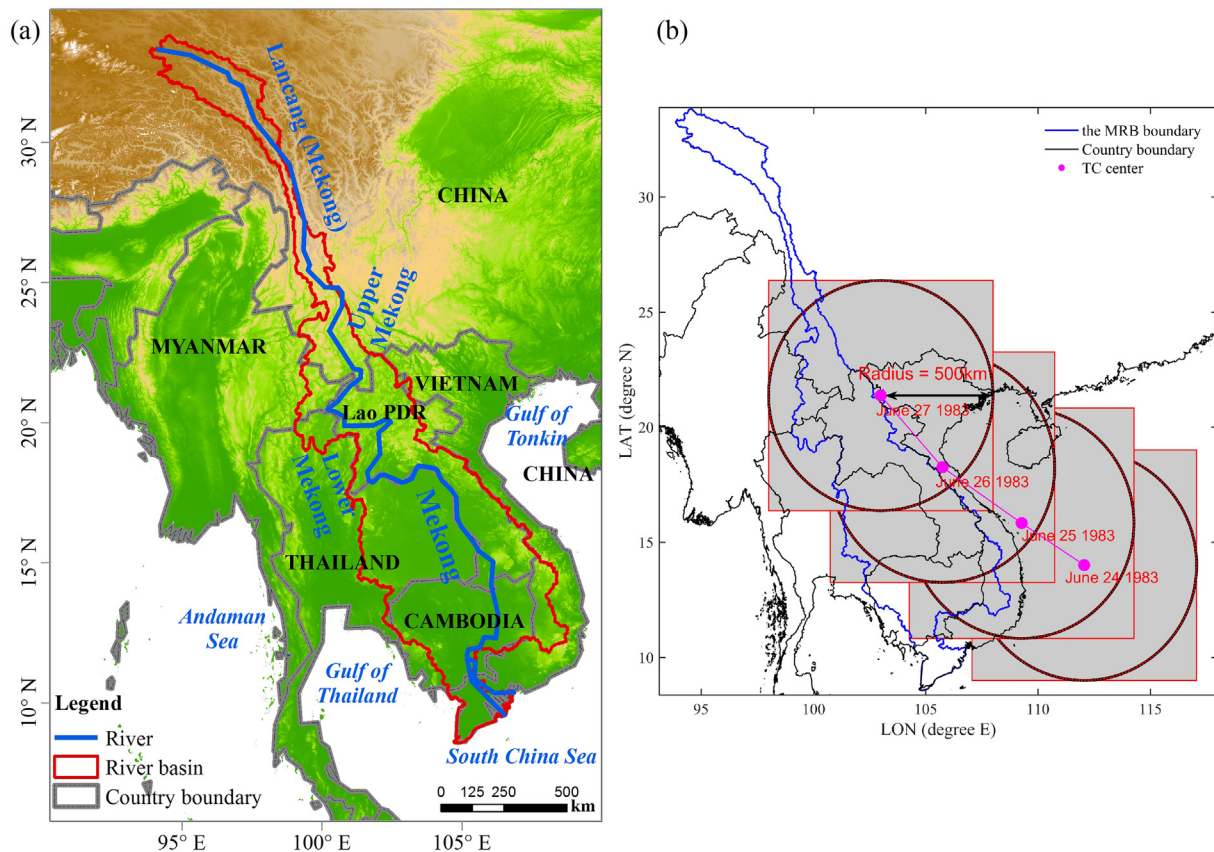


Fig. 1. (a) Terrain map of the Southeast Asia and the MRB; (b) An illustration of spatial coverage of TC on 24th -27th June 1983 across the MRB. The red dash circle is the range of 500 km radius of the TC center; and the rainfall occurs within the shaded red solid square area is considered as TCR in this study. (For interpretation of the references to colour in this figure legend, the reader is referred to the web version of this article.)

et al., 2016), the lower MRB (Chhin et al., 2016), and the MRB riparian countries (Nguyen-Thi et al., 2012a; Nguyen-Thi et al., 2012b; Takahashi et al., 2015). Though declining trends of TC frequency and TCR are observed over Indochina Peninsula during 1951–2000 (Takahashi and Yasunari, 2008), TCR contributions to total precipitation (hereafter TCRC; in %) varies at spatiotemporal scales. In Indochina Peninsula, central Vietnam is dominated by TCR (Chhin et al., 2016) with the maximum TCRC about 26% (Nguyen-Thi et al., 2012a); In the lower MRB, it occurs in Lao PDR, contributing about 20% to the annual total precipitation (Chhin et al., 2016). Moreover, in September, the TCRC can be up-to 70% over Thailand (Takahashi and Yasunari, 2008). Chhin et al. (2016) investigated the TCR in the Indochina Peninsula and lower MRB, but it only covered a short time period (i.e., 2000–2013) that falls short in studying the climatology of TCs and TCR across the MRB, especially temporal trends. Other studies relating to TCs in Indochina Peninsula, are either solely about Vietnam (Nguyen-Thi et al., 2012a,b) or Thailand (Takahashi et al., 2015). So far, studies on the long-term climatology of TCs and the TCR in the MRB basin scale have yet to be performed.

In this paper, we aim to fill this research gap by analyzing long-term climatology and trends of TCs and TCR in the MRB for 1983–2016, with the ultimate goal of better understanding the change of TCs and TCR. The purposes of this study are thus threefold: (i) to describe the climatology and trends of TCs (number, duration and intensity) on the monthly and annual basis; (ii) to quantitatively evaluate the TCR and its contribution to total precipitation both spatially and temporally; and (iii) to discuss potential mechanisms of the changing TCs and TCR.

This manuscript is structured as follows: Data and methodology are presented in Section 2; Results of the spatiotemporal climatology and trends of TCs and its contribution to the total precipitation are

described in Section 3. Section 4 discusses possible mechanisms of TCs changes. Finally, conclusions are drawn in Section 5.

2. Data and methodology

2.1. TC best-track data

TC best-track data is obtained from International Best Track Archive for Climate Stewardship (IBTrACS, <https://www.ncdc.noaa.gov/ibtracs/index.php>, last accessed 5 October 2018). In this study, we employ the latest version 3. Developed by the National Climatic Data Center (NCDC) jointly with the World Data Center of Meteorology, IBTrACS is a comprehensive worldwide collection of historical TC best-track dataset. It combines information from multiple TCs datasets, including all the Regional Specialized Meteorological Centers and Tropical Cyclone Warning Centres within the WMO, and other national agencies (Knapp et al., 2010). IBTrACS considerably facilitated analysis of global climate trends (Walsh et al., 2016), and is crucial for understanding the characteristics and impacts of TCs. A detailed description of this dataset is presented by Knapp et al. (2010). The best-track data tracks each storm at 6-h interval, and offers data of storm characteristics every six hours, such as time, longitude and latitude of storm center, type of storm, maximum sustained winds (MSW, kt), minimum central pressure (hPa). As the MRB is often influenced by TCs formed in North Indian Ocean (NIO)/ Bay of Bengal (BoB), South China Sea (SCS), and western North Pacific Ocean (WNP), here we investigate all the TCs affecting the MRB formed in the above three oceans.

2.2. Precipitation data

Facing the reality of sparsely and unevenly distributed rain gauges in the MRB (Lutz et al., 2014; MRC, 2015; Wang et al., 2016; Chen et al., 2018), we employ the Precipitation Estimation from Remote Sensing Information using an Artificial Neural Network - Climate Data Record (PERSIANN-CDR, <https://www.ncdc.noaa.gov/cdr/atmospheric/precipitation-persiann-cdr>, last accessed 5 October 2018). It is developed by the Center for Hydrometeorology and Remote Sensing at the University of California, Irvine. To estimate rainfall, PERSIANN-CDR combines infrared and passive microwave measurement information from multiple satellites by using an artificial neural network model, and a bias-adjustment with regard to the Global Precipitation Climatology Project monthly precipitation data is processed (Sorooshian et al., 2000; Ashouri et al., 2015; Huang et al., 2016). In detail, the PERSIANN-CDR offers rainfall estimates (in mm) on daily scale from 1983 to 2016, at 0.25° for the latitude band 60°N–60°S.

2.3. Climate indexes

Previous studies show that TC activity is related to the large-scale atmospheric circulation and thermodynamic structure of the atmosphere modulated by the El Niño–Southern Oscillation (ENSO) (Elsner and Liu, 2003; Ng and Chan, 2012; Walsh et al., 2016) and the Pacific Decadal Oscillation (PDO) (Camargo et al., 2010; Goh and Chan, 2010; Wang et al., 2013a). For example, the total TCs number (hereafter TCNumber) entering the SCS from the WNP are below normal under El Niño conditions but above normal under La Niña conditions (Goh and Chan, 2010; Lee et al., 2012). The ENSO index from the Golden Gate Weather Services (<http://ggweather.com/enso/oni.htm>, last accessed 5 October 2018) and the Climate Prediction Center from National Oceanic and Atmospheric Administration (NOAA, http://origin.cpc.ncep.noaa.gov/products/analysis_monitoring/ensostuff/ONI_v5.php, last accessed 5 October 2018) has been used to identify the link between ENSO and TC activity. In this study, we take the three months' mean ENSO index (December–February) for representing ENSO index in each year. Link between PDO and TC activity is investigated, by taking PDO index from Physical Sciences Division at the Earth System Research Laboratory, NOAA (http://www.esrl.noaa.gov/psd/gcos_wgsp/Timeseries/PDO/index.html, last accessed 5 October 2018). Specifically, the Pearson's correlation coefficient (r) and coefficient of determination (R^2) are employed to evaluate the correlation between the annual mean TCR and these two large-scale atmospheric circulation indexes. The r is an indicator of the degree of linear relationship between the two evaluated indexes (Moriasi et al., 2007). In short, an absolute high and significant r suggests high linkage between the two evaluated indexes over the time and vice versa.

2.4. Definition of TCR

Following previous studies (Jiang and Zipser, 2010; Khouakhi et al., 2017; Zhang et al., 2018b), the radius of 500 km from TCs center is taken as the threshold distance where all rainfall within this radius is considered as being generated by TCs. Similar to Chhin et al. (2016), we define a square box centered in the TCs center, with half side length of 500 km (i.e., 1000 km in diameter) as the influence area of the TCs. By this definition, the rainfall occurs within the box is regarded as TCR, while rainfall outside of the box is treated as none TCR. In total, we analyze 210 TCs that influenced the MRB for 1983–2016. Among them, 19 of the TCs are from NIO/BoB.

In order to measure the TCR, we first aggregate the latitudes and longitudes of the TC center from 6-h into daily interval. Then TCR is computed by each TC event's center by considering the TC radius. For example, regarding the TC event on 24th–27th June 1983, the rainfall within the box of each TC center is summed up along the track over the time (see Fig. 1b). The spatial patterns of monthly, seasonal, and annual

TCR are obtained according to the periods of interest; and then the temporal (e.g., annual, seasonal and monthly) mean TCR is averaged over the basin. Meanwhile, the spatial and temporal mean total precipitations are calculated, respectively. Finally, the TCRC at each period of interest is measured as follows (Eq. (1)):

$$TCRC = \frac{TCR}{Total\ precipitation} * 100\% \quad (1)$$

The percentage of extreme precipitation days caused by TCs to the annual total precipitation is conducted for the analysis of the influence of TCR on extreme precipitation over the basin. Here, we employ extreme precipitation indices proposed by Expert Team on Climate Change Detection, Monitoring and Indices (ETCCDMI) of the WMO: R20mm (days of heavy precipitation rate $\geq 20 \text{ mm day}^{-1}$), and R50mm (days of extremely heavy precipitation rate $\geq 50 \text{ mm day}^{-1}$) (Donat et al., 2013; Lestari et al., 2016; Imbach et al., 2018).

2.5. TC indexes and the relationship with TCR

For the purpose of understanding the link between TC indexes and TCR for 1983–2016, partial correlation coefficients between TCR and all the TC indexes in the MRB are calculated, by adjusting for the remaining TC indexes. TC indexes includes the annual TCNumber, duration of TC in hours (hereafter TCDuration), and TCs intensity (hereafter TCIntensity). We only consider the TCDuration and TCIntensity during its influencing period over the MRB, because the TCR occurs when TCs are close to the MRB. Moreover, TCIntensity is evaluated by annual/monthly mean maximum MSW (hereafter MMSW, kts; $1 \text{kt} \approx 0.51 \text{ m s}^{-1}$) over the duration. The maximum MSW over the duration of each TC event influencing the MRB is firstly derived, and then the monthly and annual MMSW are calculated.

The seasonal TCR and corresponding TCNumber in June–November and other months over the year (i.e., January–May and December) are counted respectively. The reason to study the TCR in June–November is that these months cover both monsoon season (June–October) in MRB and high TCs occurrence season (September–November) in SCS, WNP and BoB. Hereafter we named it as monsoon-TC season (i.e., June–November). Other months in the year will be named as non-monsoon-TC season.

2.6. Influence of TCs

The influence of TCs in the MRB is evaluated by: (i) TCRC both spatially and temporally; (ii) contribution of R20mm and R50mm induced by TCs to that brought by annual total precipitation; (iii) annual mean TC density (hereafter TCDensity, times yr^{-1}) defined as the number of times that the center of a TC was located within the grid by the number of observations by years (Lyon and Camargo, 2009); and (iv) annual spatial coverage of TCR. For measuring the TCDensity, we interpolate TCs best-track data (longitude and latitude) into 0.5-h interval before the calculation.

2.7. Statistic analysis

As mentioned above, the Pearson's correlation coefficient (r) is used for the correlation analysis; and partial correlation coefficient is applied to measure the linkage between each of the TC indexes and TCR over the years. Besides, the trends of TC indexes and TCR are estimated by using Sen's slope (Sen, 1968) and Mann-Kendall (Kendall, 1938), with a confidence level of 95% ($p < .05$). These methods have been widely applied in meteorological time series data (Feng and Zhou, 2012; Wu et al., 2016).

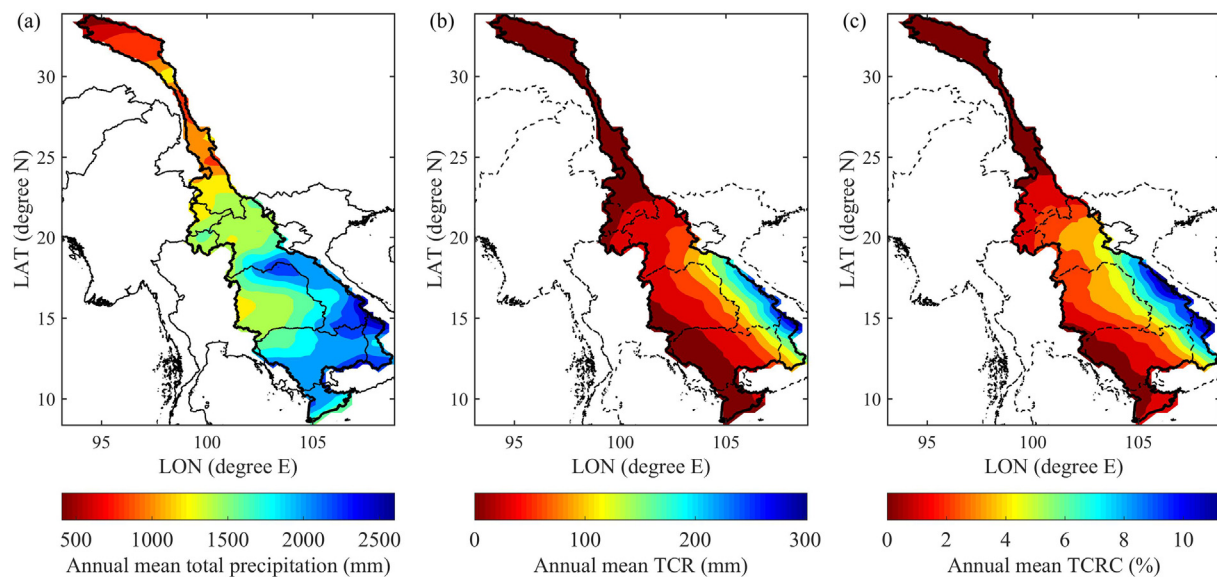


Fig. 2. Spatial patterns of annual mean (a) total precipitation (in mm), (b) TCR (in mm), and (c) TCRC (in %) across the MRB for 1983–2016.

3. Results

3.1. Climatology of the total precipitation and TCR in the MRB

The annual mean total precipitation over the MRB for 1983–2016 increases from northwest to southeast, but with two high centers in the lower MRB (Fig. 2a). The annual mean TCR mainly concentrates on the lower MRB with a spatial gradient decreasing from east to west (Fig. 2b). Specifically, the eastern lower MRB gains the largest amount of annual total precipitation and TCR to the extent of 2800 and 330 mm yr⁻¹, respectively.

The spatially averaged annual total precipitation and TCR at both annual and monthly scales in the MRB for 1983–2016 are presented in Fig. 3. On average, the annual total precipitation is about 1470 mm yr⁻¹ (ranging 1250–1700 mm yr⁻¹), and the annual TCR is 36.7 mm yr⁻¹ (ranging 5.0–73.8 mm yr⁻¹). The annual total precipitation fluctuates along the years with a non-significant trend (2.48 mm yr⁻¹, $p > .05$) during this period (Fig. 3a), but TCR displays a significant decreasing trend of -1.1 mm year⁻¹ ($p < .01$) (Fig. 3c). Based on the correlation coefficient, the annual TCR is not statistically correlated with the annual total precipitation during 1983–2016 ($r = -0.28$, $p > .05$).

Regarding the monthly distributions of the total precipitation and TCR (Fig. 3b and d), the MRB receives a large proportion of total precipitation in monsoon season summing in July–August, whereas it peaks in September–October in terms of TCR. Both of them are of unimodal distributions with different shapes. In particular, there is rare TCR during December and April, whilst high variabilities exist in the monthly mean TCR, especially in those months with higher TCR.

Fig. 4 shows the spatial patterns of annual mean contribution of TC induced extreme precipitation (R20mm and R50mm) to that from total precipitation across the MRB for 1983–2016. Results present similar spatial patterns to TCR. As to the contribution to the total precipitation, the highest contribution of TCs induced R20mm is 17.1% over the basin (Fig. 4a), but it surges to 29.6% regarding R50mm (Fig. 4b); and the area with the highest contribution is in eastern part of Lao PDR in terms of R20mm, but more southward in Vietnam for R50mm.

3.2. Climatology of TC indexes

On average, 6.2 TCs influence the MRB for 13 days per year, with the MMSW of 51.8 kt (see Fig. 5). In terms of the annual TCIntensity

indexes, the higher MMSW, the higher TCIntensity (Fig. 5c). TCNumber (-0.1 yr⁻¹, $p < .05$) and TCDuration (-6.2 h yr⁻¹, $p < .05$) display consistent trends as TCR does, with significant decreasing trends, while it is insignificant in terms of TCIntensity (MMSW: -0.1 kt yr⁻¹, $p > .05$). Overall, we find a decreasing trend of TC frequency across the MRB. Likewise, TCR is significantly correlated with the TC indexes, as results of the partial correlation coefficient shown. Specifically, TCR is highly correlated with the TCDuration ($r = 0.66$, $p < .0001$) and TCIntensity ($r = 0.41$, $p < .05$), but insignificantly with TCNumber.

Fig. 6 displays the spatially averaged TCR and TCNumber for the monsoon- and non-monsoon-TC season for 1983–2016. With 5.2 TCs per year on average, the mean TCR in monsoon-TC season is about 35.2 mm yr⁻¹ (ranging 4.2–73.8 mm yr⁻¹), corresponding to over 95% (ranging 67–100%) of the annual mean TCR. Moreover, TCR in monsoon-TC season (Fig. 6a) is significantly correlated with the annual mean TCR (Fig. 3c, $r = 0.99$, $p < .0001$), so does the TCNumber at the two time scales ($r = 0.93$, $p < .0001$). With respect to the non-monsoon-TC season, the mean TCNumber and TCR in the non-monsoon-TC season are 0.9 and 1.5 mm yr⁻¹ respectively. Non-monsoon-TC season TCR (Fig. 6c) is not correlated with the annual mean TCR, neither do TCNumbers at these two time scales.

According to the correlation coefficient for 1983–2016 in Table 1, the annual mean total precipitation is highly correlated with PDO ($r = -0.46$, $p < .01$), as well as with ENSO ($r = -0.34$, $p = .05$). On the contrary, PDO and ENSO both are insignificantly correlated with TCR, or with the TC indexes (TCNumber, TCDuration, and TCIntensity), indicating insignificant correlation between ENSO/PDO and TC activity in the MRB.

3.3. Influence of TCs and TCR in the MRB

The spatial distribution of annual mean TCRC across the MRB (Fig. 2c) displays a pattern similar to TCR (Fig. 2b), with the maximum TCRC of 12.4% in the eastern of the lower MRB. A distinct TCRC gradient is also identified from east ($\sim 12\%$) to west ($\sim 0\%$) in the lower MRB. Overall, the spatially averaged annual TCRC is 2.5% yr⁻¹ on average (ranging 0.3–5.3% yr⁻¹) (Fig. 7a) with a significant decreasing trend of -0.1% yr⁻¹ ($p < .001$), showing similar trend to the TCR (Fig. 3c) and TCNumber (Fig. 5a). At monthly scale, the TCRC has a unimodal distribution and peaks in November (Fig. 7b).

Following the tracks of TCs in the MRB, the annual mean TCDensity in the MRB over the study period is shown in Fig. 8a. The TCDensity is

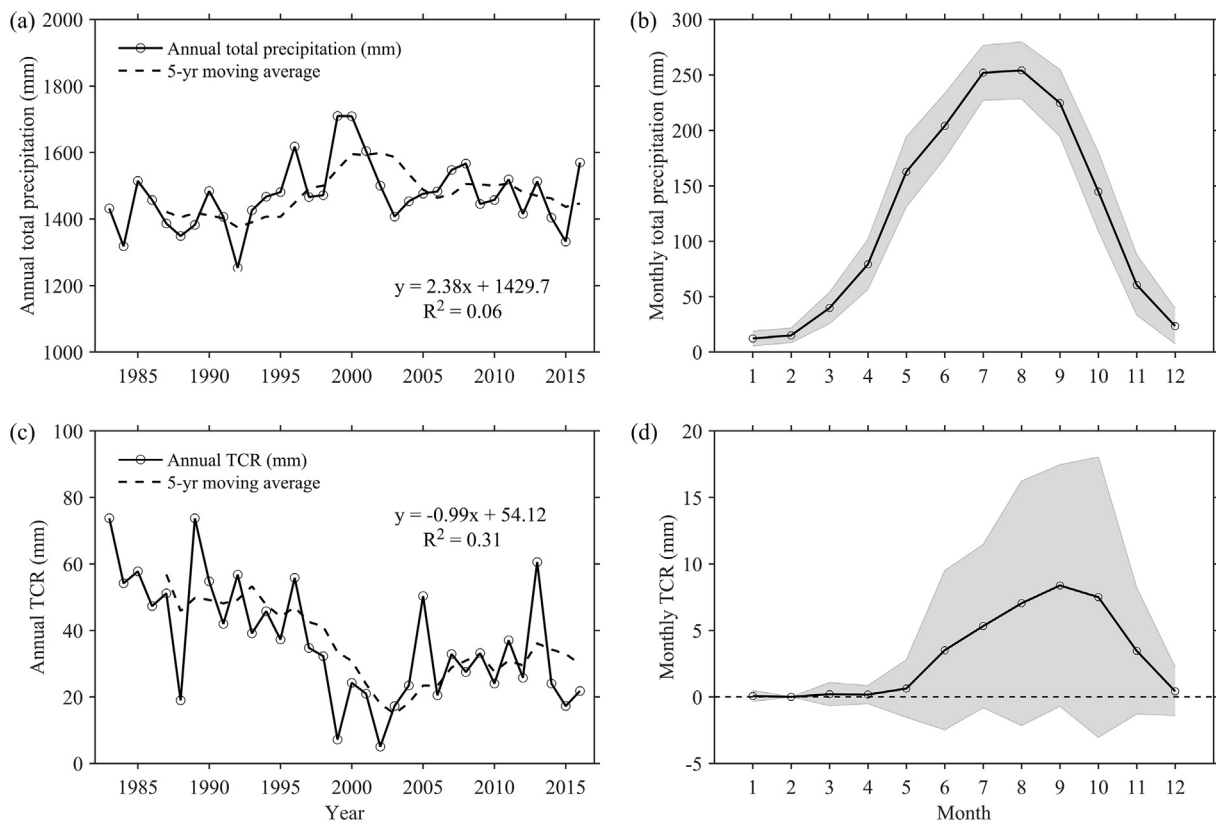


Fig. 3. Spatially averaged precipitation (in mm) across the MRB for 1983–2016. (a) Annual total precipitation; (b) Monthly mean total precipitation; (c) Annual TCR; and (d) Monthly mean TCR. Black dash line in (a) and (c) is the 5-yr moving average, and the gray shade in (b) and (d) is the range of ± 1 standard deviation. Equations shown in (a) and (c) are the linear trend regressions, respectively.

scattering in the riparian countries, with a greater density of TCs in the eastern of the lower MRB. Generally, the spatial coverage of the MRB affected by TCR for 1983–2016 at annual scale shows high variability with a mean percentage of 66.6%; while 2002 is an extreme year of the lowest TCR influence (23.9%, Fig. 8b). Similar to the TCs indexes, a significant decreasing trend exists in the spatial coverage over the years ($-0.6\% \text{ yr}^{-1}$, $p < .01$).

4. Discussion

4.1. Spatiotemporal influence of TCs in the MRB

Generally speaking, TCR contribution to the annual total precipitation is minor over the MRB for 1983–2016. As shown by our results, the spatially averaged annual mean TCRC is 2.5%, with the

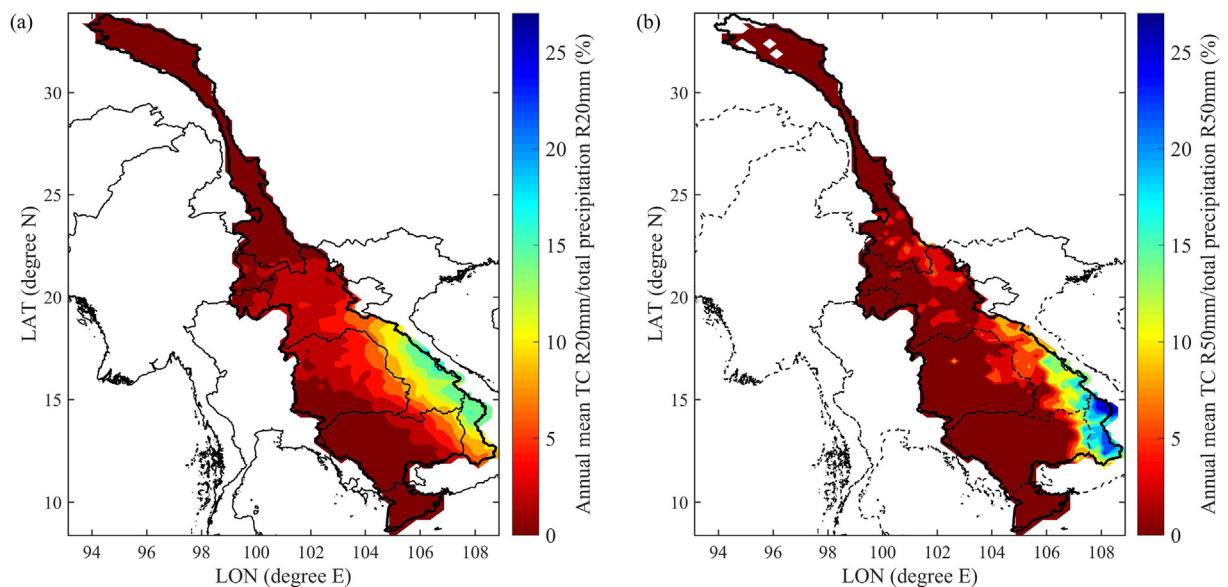


Fig. 4. Spatial patterns of annual mean contribution of TC induced (a) R20mm (b) and R50mm to that from annual total precipitation (in %) across the MRB for 1983–2016.

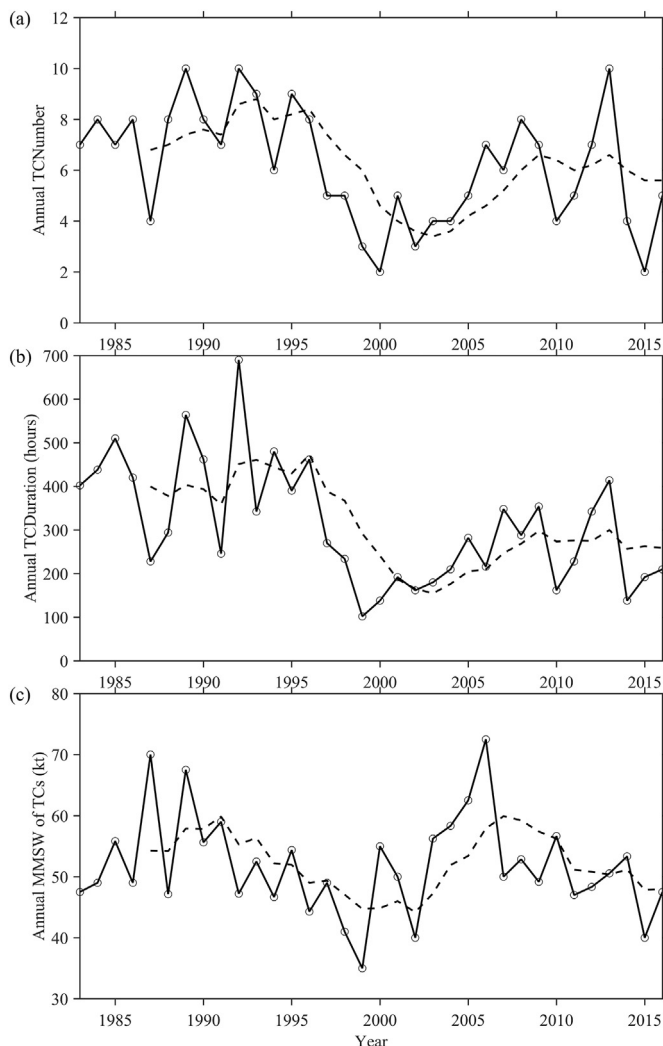


Fig. 5. Characteristics of annual TC activity across the MRB for 1983–2016. (a) TCNumber; (b) TCDuration (in hours); (c) MMSW of TCs (in kt). Black dash line in each sub-figures is the 5-yr moving average.

annual mean total precipitation and TCR of 1470 and 36.7 mm respectively. Considering the monthly TC activity, the TCs' influence across the MRB is high during August–November, coinciding with the monsoon season to a large extent, and it peaks in September–November. Since TCs formed in NIO/BoB only contribute to 9% of the TCNumber and the primarily TCR occurs in the western coast of Myanmar (Zhang et al., 2018c), TCs influencing the MRB mainly come from WNP and SCS. As previous studies concluded, the most active TC season in WNP (and SCS) is June–November, while peak months varies among July–October (Wang and Chan, 2002; Camargo and Sobel, 2005; Wang et al., 2013a; Park et al., 2014); and most of the TCs making landfall in the MRB peak in September–October (Nguyen-Thi et al., 2012a; MRC, 2015). Therefore, our results are consistent with previous results.

Given the short duration of TCs (6.2 TCs and 13 days per year) in the basin, however, TCs could seriously affect the local area along the TCs tracks by carrying extreme rainfall at short time period (Rios Gaona et al., 2018; Zhang et al., 2018b). Regarding the inner-annual distribution of TCs and TCR, high proportion of the TCs occurs in monsoon-TC season, contributing to around 95% of the annual mean TCR. Besides, a higher frequency of TC successions in September exists in Southeast Asia than elsewhere in the Tropics (MRC, 2015). Our results also show a large contribution of the extreme precipitation from TCs. Chiefly, occurring in monsoon season or just after that, short-term and

strong TC induced extreme rainfall is very effective in generating runoff (Darby et al., 2013, 2016) when it falls on the pre-wetted catchment, that could lead to extreme flooding in the MRB.

Generally, heterogeneous spatial patterns of TCs and TCR have been shown in our results, with high TCDensity concentrating on the lower basin especially in the eastern area, so that the area to the eastern are mostly affected by TCs. TCs originated from WNP or SCS penetrated into the MRB by crossing Vietnam and Southern China from the east and southeast (MRC, 2007, 2015), while TCs formed in the NIO/BoB used to make landfalling in Myanmar coast (Wang et al., 2013b). Commonly, the survival of TCs require continuous supply of moisture and energy (Bender et al., 1985; Goh and Chan, 2010). It weakens rapidly as it moves towards the inland (Rios Gaona et al., 2018), because it generates heavy rainfall by interacting with topography while much less moisture supply from the land (Bender et al., 1985; Park and Lee, 2007; MRC, 2010). The interaction with topography is also a reason of the heaving rainfall accompanied by the TCs (Park and Lee, 2007). A further study should deepen insight into the relationship between TCR and flood, particularly in the lower eastern MRB.

The risk of TCs on the society is highly concerned over the world, and many works have investigated such effects (Rappaport, 2014; Zhou and Matyas, 2017; Zhang et al., 2018a). For example, the threat of intense TCs over east China, Korea and Japan has increased in 1977–2010, because of a significant shifting to coastlines of the spatial positions of the maximum TCIntensity (Park et al., 2014). Though no clear tendency of landfall TCIntensity exists along the Vietnam coastline (Park et al., 2014), increasing TCIntensity in the BoB and an eastward TC track towards Myanmar pre-monsoon season have been observed since post-1979 (Wang et al., 2013b). Besides, TCs landfalling in the MRB are easy to result in overwhelmed hydrological hazards (e.g., flood), as well as the secondary disaster (e.g., landslides, mudslides). It could lead to loss of property and mortality in the society (Rappaport, 2000; Pielke et al., 2008; Zhou and Matyas, 2017). Since the TCIntensity and TCR are expected to increase under the warming climate scenario (Webster et al., 2005; Knutson et al., 2010; Lin et al., 2015), how will the TCs change in the next decades and how will it influence the MRB are key topics for future research.

4.2. Mechanisms for TC changes

4.2.1. (a) Relationship between TC indexes and TCR

The TCR in the MRB is dominated by the joint effects of TCNumber, TCDuration, and TCIntensity, as results shown significant correlation coefficient with TC indexes. TCNumber and TCDuration are significant factors influencing the TCR, while TCIntensity is correlated to the genesis location of TCs and the TCDuration (Park et al., 2011, Park et al., 2014). For instance, a non-significant increase of TC genesis over the northern SCS shortens its lifetime and leads to landfall intensity reduction over Vietnam. Unlike lanfalling TC in Korea and Japan (Park et al., 2011), the TCDuration is insignificant with the TCIntensity of the TCs influencing MRB.

4.2.2. (b) Possible mechanisms for the declining TCs

Our results indicate a weakening trend of the TC frequency over the study period in the MRB. Also, declining trends are observed over Indochina Peninsula for 1951–2000 (TCs and TCR occurring in September) (Takahashi and Yasunari, 2008), in the BoB (Mohapatra et al., 2012; Sahoo and Bhaskaran, 2016), and the SCS in recent decades (Lee et al., 2012; Wang et al., 2013a; Park et al., 2014).

Studies suggest that the TCs are tightly correlated with large scale atmospheric circulation, e.g., ENSO and PDO (Elsner and Liu, 2003; Jiang and Zipser, 2010; Lee et al., 2012; Walsh et al., 2016). Less TCs enter into the SCS from the WNP under El Niño conditions, and vice versa (Goh and Chan, 2010; Lee et al., 2012). Besides, the La Niña phases more strongly affect TCR than the El Niño phases (Goh and Chan, 2010; Jiang and Zipser, 2010; Nguyen-Thi et al., 2012a). TCs

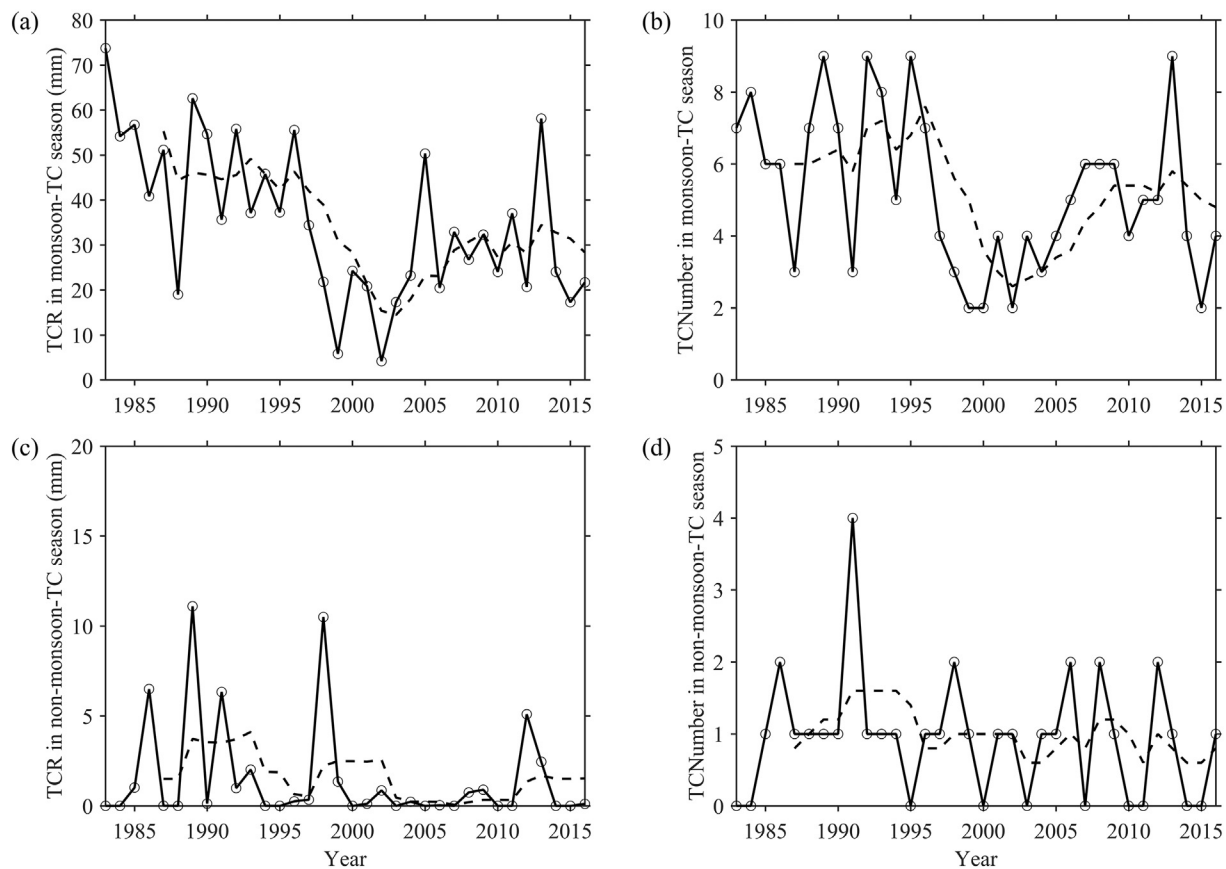


Fig. 6. Seasonally spatial averaged TCR (in mm) and TCNumber across the MRB for 1983–2016. (a) TCR and (b) TCNumber in monsoon-TC season; (c) TCR and (d) TCNumber in non-monsoon-TC season. Black dash line in each sub-figure is the 5-yr moving average.

Table 1
Correlation coefficient between atmospheric circulation and TC indexes.

Index	ENSO		PDO	
	<i>r</i>	<i>p-value</i>	<i>r</i>	<i>p-value</i>
TCNumber	−0.13	0.45	−0.04	0.83
TCDuration (entire life time)	0.06	0.73	0.20	0.25
TCDuration (when influencing MRB)	−0.01	0.95	0.09	0.62
MMSW (entire life time)	−0.1	0.59	−0.05	0.79
MMSW (when influencing MRB)	0.14	0.44	0.06	0.74
TCR	−0.01	0.93	0.18	0.30
Total precipitation	−0.34*	0.05	−0.46**	0.01

*, **: Statistically significant *r* were defined as those $p < .05$, and $p < .01$, respectively.

formed in the NIO/BoB also exhibit similar characteristics under ENSO conditions (Ng and Chan, 2012). For TCs formed inside the SCS, such difference is not as obvious (Goh and Chan, 2010). As to PDO, positive PDO generally favors less TCs, while on the contrary under negative PDO (Goh and Chan, 2010; Lee et al., 2012). Our results of the negative *r* between the ENSO/PDO and TCNumber also suggest the influence of these two atmospheric circulations on TC activity across the MRB. However, both ENSO and PDO are non-significantly correlated with the TC indexes (see Table 1).

There are two possible reasons for such declining trends. First, TCs which influence the MRB are mostly originated from WNP or SCS. Though evidences show no clear trend of TCs in the WNP (Yeh et al., 2010; Liu and Chan, 2013; Tao and Lan, 2017), there is a shifting flow of TCs originated from WNP, from straight-moving to northwestwards (Wu et al., 2005; Park et al. 2011; Lee et al., 2012). Such shifting leads to a decrease of TCs entering the SCS and its impact on the MRB (Lee

et al., 2012; Wang et al., 2013a; Park et al., 2014), whereas an enhancement of TCs trend exists in East Asia at the same time (Park et al. 2011, Park et al., 2014; Chen et al., 2013). Second, fewer number of TCs have formed over the southern part of the SCS since 1977 (Park et al., 2014), associating to the increasing sea surface temperature in the tropical Indian Ocean (Wang et al., 2013a). In addition, a decreasing trend of the post-monsoon TCs formed in the BoB since 1960s is observed (Sahoo and Bhaskaran, 2016).

4.3. Uncertainties

Two factors may have contributed to uncertainties of the results in this study. First, since the temporal resolution of precipitation dataset - PERSIANN-CDR - is on daily scale, we aggregated the 6-h interval TC best-track data into daily scale. As the TCR changes along the TC moving path (or stage), the aggregating approach applied here could bring uncertainties for the total amount of TCR. Nevertheless, the long-term PERSIANN-CDR offers precipitation with relatively high spatio-temporal resolutions (Ashouri et al., 2015; Liu et al., 2017), among those datasets that are available and has good ability in resembling the precipitation in MRB as proved recently by Chen et al. (2018). Indeed, this product makes the study of precipitation-related climatology available by satellite-retrieved precipitation at finer resolutions than previously possible (Ashouri et al., 2015; Liu et al., 2017). Second, the TCR definition used in this study is based on 500 km radius threshold. Though the radius varies in different storms and a storm in its different stage, recent studies indicate that most of the rainfall induced by TCs occurs within a radius of 500 km (Khouakhi et al., 2017), and rainfall radius changes little in regard to its intensity (Lin et al., 2015).

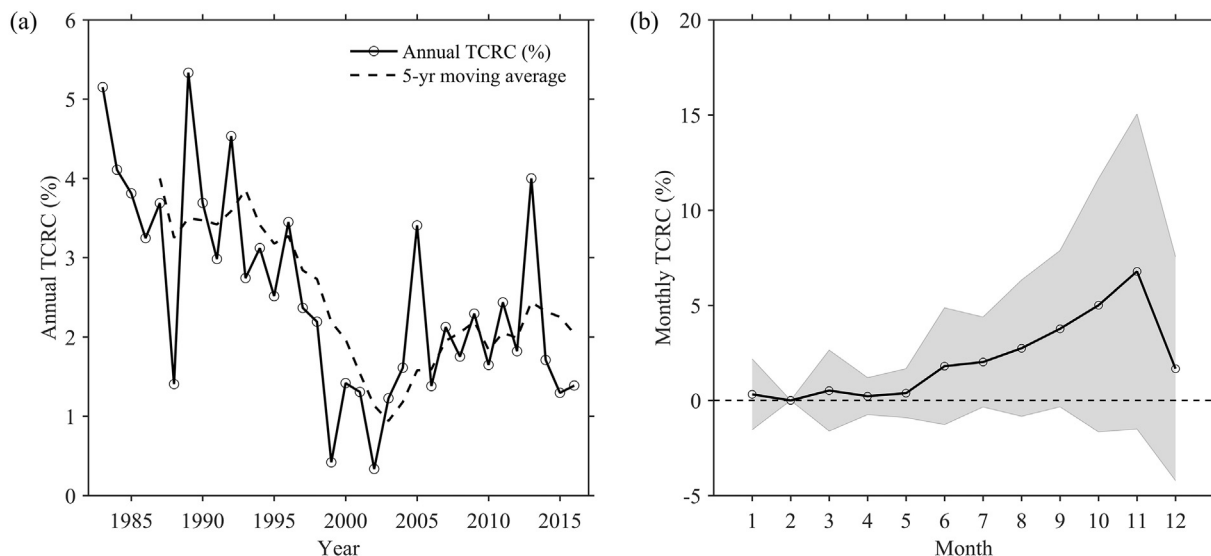


Fig. 7. Spatially averaged TCRC (in %) across the MRB for 1983–2016. (a) Annual TCRC; (b) Monthly mean TCRC. Black dash line in (a) is the 5-yr moving average, and the gray shade in (b) is the range of ± 1 standard deviation.

5. Conclusion

In this study, the climatology and trends of TCs and associated rainfall in the MRB have been investigated by using satellite data (PERSIANN-CDR) and the best-track data (IBTrACS) for 1983–2016. The results of the study can be summarized as follows:

- i. The annual mean TCNumber affecting the basin is 6.2 yr^{-1} , and the annual mean TCR is 36.7 mm yr^{-1} contributing 2.5% to the total precipitation.
- ii. TCs highly concentrate on the lower eastern MRB, leading to the largest TCR contribution to annual total precipitation of 12.4%.
- iii. The annual mean contribution of TCs induced extreme precipitation (R20mm and R50mm) to that from total precipitation is high in lower eastern MRB (17.1% and 29.6%, respectively).
- iv. On average, 66.6% of the MRB is influenced by TCR over the year.
- v. A weakening trend of the TC frequency in the MRB is observed for 1983–2016, with a significant decreasing trend of TCNumber (-0.1 yr^{-1} , $p < .05$), and TCDuration (-6.2 h yr^{-1} , $p < .05$).

This long-term climatology research in the MRB since 1980s could lay a foundation of further in-depth research of the potential influence of the dynamic of TCs and the associated rainfall in the MRB.

Acknowledgements

This research was supported by the Strategic Priority Research Program of Chinese Academy of Sciences (Grant No. XDA20060401); the China Scholarship Council; the National Natural Science Foundation of China (Grant No. 91537210); Swedish STINT (Grant No. CH2015–6226); the European Union's Horizon 2020 research and innovation programme under the Marie Skłodowska-Curie grant agreement (Grant No. 703733); and the Swedish VR (Grant No. 2017-03780). We would like to acknowledge the NCDC for providing the IBTrACS; the CHRS at the University of California, Irvine for the PERSIANN-CDR; the Golden Gate Weather Services for the ENSO data; and the Climate Prediction Center-National Centers for Environmental Prediction, the Earth System Research Laboratory, and NOAA for the PDO.

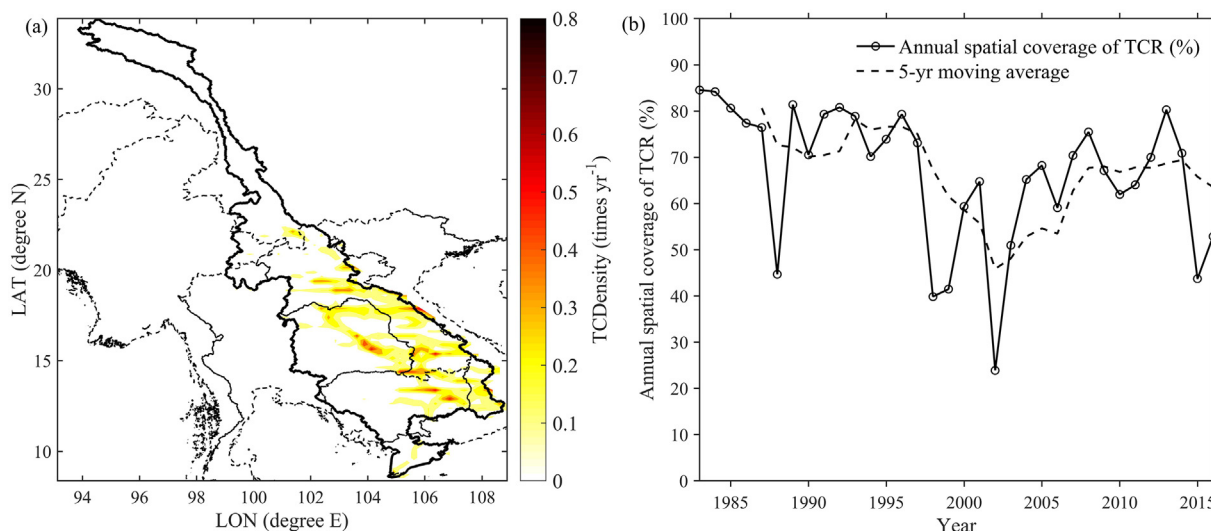


Fig. 8. (a) Spatial patterns of annual mean TCDensity (times yr^{-1}) and (b) annual spatial coverage of TCR (in %) across the MRB for 1983–2016. Black dash line is the 5-yr moving average.

References

- Ashouri, H., Hsu, K.L., Sorooshian, S., et al., 2015. PERSIANN-CDR: Daily precipitation climate data record from multisatellite observations for hydrological and climate studies. *Bull. Am. Meteorol. Soc.* 96, 69–83. <https://doi.org/10.1175/BAMS-D-13-00068.1>.
- Bender, M.A., Tuleya, R.E., Kurihara, Y., 1985. A numerical study of the effect of a mountain range on a landfalling tropical cyclone. *Mon. Weather Rev.* 113, 567–582.
- Camargo, S.J., Sobel, A.H., 2005. Western North Pacific tropical cyclone intensity and ENSO. *J. Clim.* 18, 2996–3006. <https://doi.org/10.1175/JCLI3457.1>.
- Camargo, S.J., Sobel, A.H., Barnston, A.G., Klotzbach, P.J., 2010. The influence of natural climate variability on tropical cyclones and seasonal forecasts of tropical cyclone activity. In: *Glob Perspect Trop Cyclones, From Sci to Mitig*, pp. 325–360.
- Chen, J.M., Chen, H.S., Liu, J.S., 2013. Coherent interdecadal variability of tropical cyclone rainfall and seasonal rainfall in Taiwan during October. *J. Clim.* 26, 308–321. <https://doi.org/10.1175/JCLI-D-11-00697.1>.
- Chen, A., Chen, D., Azorin-Molina, C., 2018. Assessing reliability of precipitation data over the Mekong River Basin: a comparison of ground-based, satellite, and reanalysis datasets. *Int. J. Climatol.* <https://doi.org/10.1002/joc.5670>. In press.
- Chhin, R., Trilaksono, N.J., Hadi, T.W., 2016. Tropical cyclone rainfall structure affecting Indochina peninsula and lower Mekong river basin (LMB). *J. Phys. Conf. Ser.* 739. <https://doi.org/10.1088/1742-6596/739/1/012103>.
- Darby, S.E., Leyland, J., Kumm, M., et al., 2013. Decoding the drivers of bank erosion on the Mekong river: the roles of the Asian monsoon, tropical storms, and snowmelt. *Water Resour. Res.* 49, 2146–2163. <https://doi.org/10.1002/wrcr.20205>.
- Darby, S.E., Hackney, C.R., Leyland, J., et al., 2016. Fluvial sediment supply to a megadelta reduced by shifting tropical-cyclone activity. *Nature* 539, 276–279. <https://doi.org/10.1038/nature19809>.
- Dare, R.A., Davidson, N.E., McBride, J.L., 2012. Tropical Cyclone Contribution to Rainfall over Australia. *Mon. Weather Rev.* 140, 3606–3619. <https://doi.org/10.1175/MWR-D-11-00340.1>.
- Donat, M.G., Alexander, L.V., Yang, H., et al., 2013. Updated analyses of temperature and precipitation extreme indices since the beginning of the twentieth century: the HadEX2 dataset. *J. Geophys. Res. Atmos.* 118, 2098–2118. <https://doi.org/10.1002/jgrd.50150>.
- Elsner, J.B., Liu, K.B., 2003. Examining the ENSO-typhoon hypothesis. *Clim. Res.* 25, 43–54. <https://doi.org/10.3354/cr025043>.
- Erban, L.E., Gorelick, S.M., Zebker, H.A., 2014. Groundwater extraction, land subsidence, and sea-level rise in the Mekong Delta, Vietnam. *Environ. Res. Lett.* 9. <https://doi.org/10.1088/1748-9326/9/8/084010>.
- Feng, L., Zhou, T., 2012. Water vapor transport for summer precipitation over the Tibetan Plateau: Multidata set analysis. *J. Geophys. Res. Atmos.* 117, 1–16. <https://doi.org/10.1029/2011JD017012>.
- Goh, A.Z.C., Chan, J.C.L., 2010. Interannual and interdecadal variations of tropical cyclone activity in the South China Sea. *Int. J. Climatol.* 30, 827–843. <https://doi.org/10.1002/joc.1943>.
- Huang, A., Zhao, Y., Zhou, Y., et al., 2016. Evaluation of multisatellite precipitation products by use of ground-based data over China. *J. Geophys. Res. Atmos.* 121, 10654–10675. <https://doi.org/10.1002/2016JD025456>.
- Imbach, P., Chou, S.C., Lyra, A., et al., 2018. Future climate change scenarios in Central America at high spatial resolution. *PLoS One* 13, 1–21. <https://doi.org/10.1371/journal.pone.0193570>.
- Jiang, H., Zipser, E.J., 2010. Contribution of tropical cyclones to the global precipitation from eight seasons of TRMM data: regional, seasonal, and interannual variations. *J. Clim.* 23, 1526–1543. <https://doi.org/10.1175/2009JCLI3303.1>.
- Kendall, M.G., 1938. A new measure of rank correlation. *Biometrika* 30, 81. <https://doi.org/10.2307/2332226>.
- Khouakhi, A., Villarini, G., Vecchi, G.A., 2017. Contribution of tropical cyclones to rainfall at the global scale. *J. Clim.* 30, 359–372. <https://doi.org/10.1175/JCLI-D-16-0298.1>.
- Knapp, K.R., Kruk, M.C., Levinson, D.H., et al., 2010. The international best track archive for climate stewardship (Ibtracs) unifying tropical cyclone data. *Bull. Am. Meteorol. Soc.* 91, 362. <https://doi.org/10.1175/2009BAMS2755.1>.
- Knutson, T.R., McBride, J.L., Chan, J., et al., 2010. Tropical cyclones and climate change. *Nat. Geosci.* 3, 157–163. <https://doi.org/10.1038/ngeo779>.
- Lee, T.C., Leung, C.Y.Y., Kok, M.H., Chan, H.S., 2012. The long term variations of tropical cyclone activity in the South China Sea and the vicinity of Hong Kong. *Trop Cyclone Res Rev* 1, 277–292. <https://doi.org/10.6057/2012TCRR02.01>.
- Lestari, S., Hamada, J.-I., Syamsudin, F., et al., 2016. ENSO Influences on Rainfall Extremes around Sulawesi and Maluku Islands in the Eastern Indonesian Maritime Continent. *Sola* 12, 37–41. <https://doi.org/10.2151/sola.2016-008>.
- Lin, Y., Zhao, M., Zhang, M., 2015. Tropical cyclone rainfall area controlled by relative sea surface temperature. *Nat. Commun.* 6, 1–7. <https://doi.org/10.1038/ncomms7591>.
- Liu, K.S., Chan, J.C.L., 2013. Inactive period of Western North Pacific tropical cyclone activity in 1998–2011. *J. Clim.* 26, 2614–2630. <https://doi.org/10.1175/JCLI-D-12-00053.1>.
- Liu, X., Yang, T., Hsu, K., et al., 2017. Evaluating the streamflow simulation capability of PERSIANN-CDR daily rainfall products in two river basins on the Tibetan Plateau. *Hydrol. Earth Syst. Sci.* 21, 169–181. <https://doi.org/10.5194/hess-21-169-2017>.
- Lutz, A., Terink, W., Droogers, P., et al., 2014. Development of Baseline Climate Data Set and Trend Analysis in the Mekong Basin. Wageningen, The Netherlands.
- Lyon, B., Camargo, S.J., 2009. The seasonally-varying influence of ENSO on rainfall and tropical cyclone activity in the Philippines. *Clim. Dyn.* 32, 125–141. <https://doi.org/10.1007/s00382-008-0380-z>.
- Martin, U., 2015. Health after disaster: a perspective of psychological/health reactions to disaster. *Cogent Psychol* 2. <https://doi.org/10.1080/23311908.2015.1053741>.
- Mohapatra, M., Bandyopadhyay, B.K., Tyagi, A., 2012. Best track parameters of tropical cyclones over the North Indian Ocean: a review. *Nat. Hazards* 63, 1285–1317. <https://doi.org/10.1007/s11069-011-9935-0>.
- Moriyas, D.N., Arnold, J.G., Van Liew, M.W., et al., 2007. Model evaluation guidelines for systematic quantification of accuracy in watershed simulations. *Trans. ASABE* 50, 885–900.
- MRC, 2007. Annual Mekong Flood Report 2006. Mekong River Commission, Vientiane, Lao PDR.
- MRC, 2010. State of the Basin Report 2010. Mekong River Commission, Vientiane, Lao PDR.
- MRC, 2015. Annual Mekong Flood Report 2013. Mekong River Commission, Vientiane, Lao PDR.
- Ng, E.K.W., Chan, J.C.L., 2012. Interannual variations of tropical cyclone activity over the north Indian Ocean. *Int. J. Climatol.* 32, 819–830. <https://doi.org/10.1002/joc.2304>.
- Nguyen, H.N., 2008. Human Development Report 2007/2008 Flooding in Mekong River Delta, Viet Nam.
- Nguyen-Thi, H.A., Matsumoto, J., Ngo-Duc, T., Endo, N., 2012a. A Climatological Study of Tropical Cyclone Rainfall in Vietnam. *Sola* 8, 41–44. <https://doi.org/10.2151/sola.2012-011>.
- Nguyen-Thi, H.A., Matsumoto, J., Thanh, N., Endo, N., 2012b. Long-term trends in tropical cyclone rainfall in Vietnam. *ISSN 1995-6983. J. Agrofor Environ* 6, 89–92.
- Park, D.-S.R., Ho, C.-H., Kim, J.-H., Kim, H.-S., 2011. Strong landfall typhoons in Korea and Japan in a recent decade. *J. Geophys. Res.* 116. <https://doi.org/10.1029/2010JD014801>. D07105.
- Park, S.K., Lee, E., 2007. Synoptic features of orographically enhanced heavy rainfall on the east coast of Korea associated with Typhoon Rusa (2002). *Geophys. Res. Lett.* 34, 1–5. <https://doi.org/10.1029/2006GL028592>.
- Park, D.S.R., Ho, C.H., Kim, J.H., 2014. Growing threat of intense tropical cyclones to East Asia over the period 1977–2010. *Environ. Res. Lett.* 9. <https://doi.org/10.1088/1748-9326/9/1/014008>.
- Pielke Jr., R.A., Gratz, J., Landsea, C.W., et al., 2008. Normalized hurricane damage in the United States: 1900–2005. *Nat Hazards Rev* 9, 29–42. [https://doi.org/10.1061/\(ASCE\)1527-6988\(2008\)9:1\(29\)](https://doi.org/10.1061/(ASCE)1527-6988(2008)9:1(29)).
- Rappaport, E.N., 2000. Loss of life in the {United States} associated with recent {Atlantic} tropical cyclones. *Bull. Am. Meteorol. Soc.* 81, 2065–2073. [https://doi.org/10.1175/1520-0477\(2000\)081<2065:LOLITU>2.3.CO;2](https://doi.org/10.1175/1520-0477(2000)081<2065:LOLITU>2.3.CO;2).
- Rappaport, E.N., 2014. Fatalities in the United States from Atlantic tropical cyclones: New data and interpretation. *Bull. Am. Meteorol. Soc.* 95, 341–346. <https://doi.org/10.1175/BAMS-D-12-00074.1>.
- Räsänen, T.A., Kumm, M., 2013. Spatiotemporal influences of ENSO on precipitation and flood pulse in the Mekong River Basin. *J. Hydrol.* 476, 154–168. <https://doi.org/10.1016/j.jhydrol.2012.10.028>.
- Rios Gaona, M.F., Villarini, G., Zhang, W., Vecchi, G.A., 2018. The added value of IMERG in characterizing rainfall in tropical cyclones. *Atmos. Res.* 209, 95–102. <https://doi.org/10.1016/j.atmosres.2018.03.008>.
- Sahoo, B., Bhaskaran, P.K., 2016. Assessment on historical cyclone tracks in the Bay of Bengal, east coast of India. *Int. J. Climatol.* 109, 95–109. <https://doi.org/10.1002/joc.4331>.
- Sen, P.K., 1968. Estimates of the regression coefficient based on Kendall's Tau. *J. Am. Stat. Assoc.* 63, 1379–1389. <https://doi.org/10.1080/01621459.1968.10480934>.
- Sorooshian, S., Hsu, K.L., Gao, X., et al., 2000. Evaluation of PERSIANN system satellite-based estimates of tropical rainfall. *Bull. Am. Meteorol. Soc.* 81, 2035–2046. [https://doi.org/10.1175/1520-0477\(2000\)081<2035:EOPSS>2.3.CO;2](https://doi.org/10.1175/1520-0477(2000)081<2035:EOPSS>2.3.CO;2).
- Takahashi, H.G., Yasunari, T., 2008. Decreasing trend in rainfall over Indochina during the late summer monsoon: impact of tropical cyclones. *J. Meteorol Soc Japan* 86, 429–438.
- Takahashi, H.G., Fujinami, H., Yasunari, T., et al., 2015. Role of tropical cyclones along the monsoon trough in the 2011 Thai flood and interannual variability. *J. Clim.* 28, 1465–1476. <https://doi.org/10.1175/JCLI-D-14-00147.1>.
- Tao, L., Lan, Y., 2017. Inter-decadal change of the inter-annual relationship between the frequency of intense tropical cyclone over the western North Pacific and ENSO. *Int. J. Climatol.* 37, 4880–4895. <https://doi.org/10.1002/joc.5129>.
- Walsh, K.J.E., McBride, J.L., Klotzbach, P.J., et al., 2016. Tropical cyclones and climate change. *Wiley Interdiscip. Rev. Clim. Chang.* 7, 65–89. <https://doi.org/10.1002/wcc.371>.
- Wang, B., Chan, J.C.L., 2002. How strong ENSO events affect tropical storm activity over the western North Pacific. *J. Clim.* 15, 1643–1658. [https://doi.org/10.1175/1520-0442\(2002\)015<1643:HSEAT>2.0.CO;2](https://doi.org/10.1175/1520-0442(2002)015<1643:HSEAT>2.0.CO;2).
- Wang, L., Huang, R., Wu, R., 2013a. Interdecadal variability in tropical cyclone frequency over the South China Sea and its association with the Indian Ocean sea surface temperature. *Geophys. Res. Lett.* 40, 768–771. <https://doi.org/10.1002/grl.50171>.
- Wang, S., Buckley, B.M., Yoon, J., Fosu, B., 2013b. Intensification of premonsoon tropical cyclones in the Bay of Bengal and its impacts on Myanmar. *J. Geogr Res Atmos* 118, 4373–4384. <https://doi.org/10.1002/jgrd.50396>.
- Wang, W., Lu, H., Yang, D., et al., 2016. Modelling hydrologic processes in the Mekong River basin using a distributed model driven by satellite precipitation and rain gauge observations. *PLoS One* 11, 1–19. <https://doi.org/10.1371/journal.pone.0152229>.
- Webster, P.J., Holland, G.J., Curry, J.A., Chang, H.-R., 2005. Changes in Tropical Cyclone Number, Duration, and Intensity in a Warming Environment. *Science* 309, 1844–1846. <https://doi.org/10.1126/science.11114.1951.006.a.x>.
- WMO, 2014. Atlas of Mortality and Economic Losses from Weather, Climate and Water Extremes, 1970 to 2012. Geneva, Switzerland.
- Wu, L., Wang, B., Geng, S., 2005. Growing typhoon influence on east Asia. *Geophys. Res. Lett.* 32, 1–4. <https://doi.org/10.1029/2005GL022937>.

- Wu, F., Wang, X., Cai, Y., Li, C., 2016. Spatiotemporal analysis of precipitation trends under climate change in the upper reach of Mekong River basin. *Quat. Int.* 392, 137–146. <https://doi.org/10.1016/j.quaint.2013.05.049>.
- Yeh, S.W., Kang, S.K., Kirtman, B.P., et al., 2010. Decadal change in relationship between western North Pacific tropical cyclone frequency and the tropical Pacific SST. *Meteorog. Atmos. Phys.* 106, 179–189. <https://doi.org/10.1007/s00703-010-0057-0>.
- Zhang, Q., Gu, X., Shi, P., Singh, V.P., 2017. Impact of tropical cyclones on flood risk in southeastern China: Spatial patterns, causes and implications. *Glob Planet Change* 150, 81–93. <https://doi.org/10.1016/j.gloplacha.2017.02.004>.
- Zhang, Q., Gu, X., Li, J., et al., 2018a. The impact of tropical cyclones on extreme precipitation over coastal and Inland Areas of China and its association to ENSO. *J. Clim.* 31, 1865–1880. <https://doi.org/10.1175/JCLI-D-17-0474.1>.
- Zhang, Q., Lai, Y., Gu, X., et al., 2018b. Tropical cyclonic rainfall in China: changing properties, seasonality, and causes. *J. Geophys. Res. Atmos.* 123, 4476–4489. <https://doi.org/10.1029/2017JD028119>.
- Zhang, W., Villarini, G., Vecchi, G.A., Murakami, H., 2018c. Rainfall from tropical cyclones : high-resolution simulations and seasonal forecasts. *Clim. Dyn.* <https://doi.org/10.1007/s00382-018-4446-2>.
- Zhou, Y., Matyas, C.J., 2017. Spatial characteristics of storm-total rainfall swaths associated with tropical cyclones over the Eastern United States. *Int. J. Climatol.* 37, 557–569. <https://doi.org/10.1002/joc.5021>.
- Ziv, G., Baran, E., Nam, S., et al., 2012. Trading-off fish biodiversity, food security, and hydropower in the Mekong River Basin. *Proc. Natl. Acad. Sci.* 109, 5609–5614. <https://doi.org/10.1073/pnas.1201423109>.
- ENSO*: El Niño-Southern Oscillation
ETCCDMI: Expert Team on Climate Change Detection, Monitoring and Indices
IBTrACS: International Best Track Archive for Climate Stewardship
MMSW: Annual/monthly maximum MSW
monsoon-TC season: June–November
MRB: Mekong River Basin
MSW: Maximum sustained winds
NCDC: The National Climatic Data Center
NOAA: National Oceanic and Atmospheric Administration
non-monsoon-TC season: January–May and December
NIO: North Indian Ocean
PDO: The Pacific Decadal Oscillation
PERSIANN-CDR: The Precipitation Estimation from Remote Sensing Information using an Artificial Neural Network - Climate Data Record
R20mm: Days of heavy precipitation rate $\geq 20 \text{ mm day}^{-1}$
R50mm: Days of extremely heavy precipitation rate $\geq 50 \text{ mm day}^{-1}$
SCS: South China Sea
TCDensity: The annual mean TC density
TCDuration: The duration of TC in hours
TCIntensity: TCs intensity
TCNumber: The annual TCs numbers
TCR: TC associated rainfall
TCRC: The contribution of TCR to the total precipitation
TCs: Tropical cyclones
WNP: western North Pacific Ocean
WMO: The World Meteorological Organization

Glossary

BoB: Bay of Bengal